

SUPPORTING INFORMATION FOR:

**Crowded Bis Ligand Complexes of $\text{Ttz}^{\text{Ph,Me}}$ with First Row Transition Metals Rearrange
due to Ligand Field Effects: Structural and Electronic Characterization**

($\text{Ttz}^{\text{Ph,Me}}$ = tris(3-phenyl-5-methyl-1,2,4-triazolyl)borate)

Shannon N. Oseback,^{†,‡} Sarah W. Shim,^{†,‡} Mukesh Kumar,^{†,‡} Samuel M. Greer,[§] Sean R.
Gardner,[†] Keisha M. Lemar,[†] Paul DeGregory,[†] Elizabeth T. Papish,^{†*} David L. Tierney,[§]
Matthias Zeller,[#] Glenn P. A. Yap^{||}

Departments of Chemistry, Drexel University, 3141 Chestnut St., Philadelphia, PA 19104,

Miami University, 701 East High Street, Oxford, OH 45056,

Youngstown State University, 1 University Plaza, Youngstown OH 44555

University of Delaware, Newark, DE 19716

*Corresponding author. Tel.: 215-895-2666. E-mail: elizabeth.papish@drexel.edu

[‡]The first three authors contributed equally to this work.

[†]Drexel University

[§]Miami University

[#]Youngstown State University

^{||}University of Delaware

Table of Contents		Pages
Tables SI-1 and SI-2	Crystallographic data.....	3-4
Figure SI-1	Molecular diagram of $(\text{Ttz}^{\text{Ph,Me}})\text{ZnBr}$ (3) $\cdot 0.5\text{CH}_3\text{OH}$	5
Figure SI-2	Molecular diagram of $(\text{Ttz}^{\text{Ph,Me}})_2\text{Zn}$ (1_{Zn}).....	6
Figure SI-3	View down the B-M-B axis of various Ttz complexes.....	7
Figure SI-4	Temperature dependent NMR of $(\text{Ttz}^{\text{Ph,Me}*})\text{Ni}(\text{Ttz}^{\text{Ph,Me}})$	8
Figure SI-5	Molecular diagram of $(\text{Ttz}^{\text{Ph,Me}})_2\text{Fe}$ (1_{Fe}).....	9
Figure SI-6	Molecular diagram of $(\text{Ttz}^{\text{Ph,Me}})_2\text{Mn}$ (1_{Mn}).....	10
Figure SI-7	Coordination environment around the metal in $(\text{Ttz}^{\text{Ph,Me}})_2\text{M}$	11
Figures SI-8-10	Comparison of predicted and observed powder patterns.....	12-14

Table SI-1. Crystallographic Data for $M(\text{Ttz}^{\text{Ph,Me}})_2$ ($\mathbf{1}_M$, $M = \text{Zn, Cu, Ni, Co, Fe, Mn}$).

	$\mathbf{1}_{\text{Zn}}$	$\mathbf{1}_{\text{Cu}}$	$\mathbf{1}_{\text{Ni}}$	$\mathbf{1}_{\text{Co}}$	$\mathbf{1}_{\text{Fe}}$	$\mathbf{1}_{\text{Mn}}$
formula	$\text{C}_{54}\text{H}_{50}\text{B}_2\text{N}_{18}\text{Zn}$	$\text{C}_{54}\text{H}_{50}\text{B}_2\text{CuN}_{18}$	$\text{C}_{54}\text{H}_{50}\text{B}_2\text{NiN}_{18}$	$\text{C}_{54}\text{H}_{50}\text{B}_2\text{CoN}_{18}$	$\text{C}_{54}\text{H}_{50}\text{B}_2\text{FeN}_{18}$	$\text{C}_{54}\text{H}_{50}\text{B}_2\text{MnN}_{18}$
Fw	1038.11	1036.28	1031.43	1031.67	1028.59	1027.68
color /habit	colorless block	red block	green block	pink block	colorless block	colorless block
crystal system	trigonal	monoclinic	trigonal	trigonal	trigonal	trigonal
space group	$R\bar{3}c$	$C2/c$	$R\bar{3}c$	$R\bar{3}c$	$R\bar{3}c$	$R\bar{3}c$
$a/\text{Å}$	13.9305(3)	24.899(3)	13.9385(9)	13.8978(15)	13.9034(4)	13.8711(8)
$b/\text{Å}$	13.9305(3)	13.9223(18)	13.9385(9)	13.8978	13.9034(4)	13.8711(8)
$c/\text{Å}$	43.3326(18)	16.092(2)	43.155(6)	43.178(5)	43.507(3)	43.853(5)
α/deg	90	90	90	90	90	90
β/deg	90	120.3208(19)	90	90	90	90
γ/deg	120	90	120	120	120	120
$V/\text{Å}^3$	7282.5(4)	4815.2(11)	7261.0(12)	7222.5(12)	7283.4(5)	7307.2(11)
Z	6	4	6	6	6	6
$D_{\text{calcd}}/\text{gcm}^{-3}$	1.420	1.429	1.415	1.423	1.407	1.401
μ (mm^{-1})	0.567	0.515	0.462	0.418	0.371	0.332
$F(000)$	3240	2156	3228	3222	3216	3210
crystal dimens (mm)	0.45×0.43×0.25	0.37×0.33×0.31	0.55×0.50×0.33	0.55×0.50×0.33	0.55×0.49×0.43	0.45×0.40×0.10
θ (deg)	1.93-28.27	1.74-28.28	2.53-30.58	2.53-29.20	2.52-31.31	2.52-31.40
Rint	0.0219	0.0510	0.0388	0.0348	0.0248	0.0506
No. of measd reflections	13581	36501	9297	6495	6475	14357
No. of obsd reflections	2017	6518	2004	1997	2010	2031
GOF	1.060	1.033	1.034	1.034	1.042	1.069
Final R indices [$I > 2\sigma I$] R_1 (%) ^a , wR_2 (%) ^a	2.97, 8.06	3.82, 8.75	3.78, 10.02	3.94, 9.63	3.36, 8.58	3.78, 9.35

^aQuantity minimized = $R(wF^2) = \{\Sigma[w(F_o^2 - F_c^2)^2]/\Sigma(wF_o^2)^{21/2}\}^{1/2}$; $R(F) = \Sigma\Delta/\Sigma(F_o)$,
 $\Delta = |(F_o - F_c)|$; $w = [\sigma^2(F_o^2) + (aP)^2 + bP]^{-1}$; $P = [2F_c^2 + \text{Max}(F_o, 0)]/3$

Table SI-2. Crystallographic Data for $\text{Cu}(\text{Ttz}^{\text{Ph,Me}*})_2$ (**1_{Cu*}**),
 $(\text{Ttz}^{\text{Ph,Me}*})\text{Ni}(\text{Ttz}^{\text{Ph,Me}}) \cdot 1.16\text{CH}_2\text{Cl}_2 \cdot 0.50\text{C}_6\text{H}_{14} \cdot 0.50\text{H}_2\text{O}$ (**1_{Ni*}·solvents**), $(\text{Ttz}^{\text{Ph,Me}})\text{Ni}(\text{OH}_2)\text{Cl}$ (**2**),
 $(\text{Ttz}^{\text{Ph,Me}})\text{ZnBr} \cdot 0.5\text{CH}_3\text{OH}$ (**3_{½CH3OH}**) and $(\text{Ttz}^{\text{Me,Me}})_2\text{Co} \cdot 2\text{CH}_2\text{Cl}_2$ (**5_{2CH2Cl2}**).

	1_{Cu*}	1_{Ni*}·solvents^a	2	3_{½CH3OH}	5_{2CH2Cl2}
formula	$\text{C}_{54}\text{H}_{50}\text{B}_2\text{CuN}_{18}$	$\text{C}_{54}\text{H}_{50}\text{B}_2\text{N}_{18}\text{Ni}, \text{CH}_2\text{Cl}_2$	$\text{C}_{27}\text{H}_{27}\text{BCIN}_9$ NiO	$2(\text{C}_{27}\text{H}_{25}\text{BBrN}_9\text{Zn}), \text{CH}_4\text{O}$	$\text{C}_{26}\text{H}_{42}\text{B}_2\text{Cl}_4$ Co N ₁₈
Fw	1036.29	1116.38	598.55	1295.34	829.13
color /habit	green plate	blue block	brown plate	colorless plate	yellow block
crystal system	triclinic	monoclinic	monoclinic	trigonal	triclinic
space group	$P\bar{1}$	$C2/c$	$P2_1/n$	$P\bar{3}$	$P\bar{1}$
a/Å	10.177(2)	37.1971(18)	12.1457(10)	10.952(3)	10.5094(16)
b/Å	10.959(2)	13.2418(6)	16.6085(13)	10.952(3)	10.5276(17)
c/Å	11.986(2)	25.1526(12)	13.3465(10)	13.883(4)	19.314(4)
α/deg	67.639(6)	90	90	90	101.173(3)
β/deg	86.395(5)	107.4116(7)	90.630(2)	90	96.336(3)
γ/deg	77.426(5)	90	90	120	114.198(2)
V/Å ³	1206.3(4)	11821.4(10)	2692.1(4)	1442.1(7)	1868.7(6)
Z	1	8	4	1	2
D _{calcd} /gcm ⁻³	1.426	1.255	1.477	1.492	1.474
μ (mm ⁻¹)	0.514	0.471	0.860	2.273	0.793
F (000)	539	4640	1240	658	858
crystal dimens (mm)	0.37×0.33×0.10	0.55×0.50×0.45	0.30×0.22×0.08	0.31×0.27×0.11	0.41×0.39×0.27
θ (deg)	2.58-31.33	2.27-31.35	2.25-29.47	2.15-28.31	1.10-31.51
Rint	0.0337	0.0261	0.0465	0.0327	0.0340
No. of measd reflections	12510	45740	17561	20009	42736
No. of obsd reflections	5928	17863	6615	2421	11342
GOF	1.049	1.072	1.037	1.058	1.065
Final R indices [I>2σI] R ₁ (%) ^b , wR ₂ (%) ^b	4.75, 10.42	4.09, 10.65	5.43, 12.58	2.74, 6.96	5.93, 16.48

^a Additional disordered solvent is present in the structure of **1_{Ni*}·solvents**. The data were corrected using back-Fourier transform methods (Squeeze)

^b Quantity minimized = $R(wF^2) = \{\sum[w(F_o^2 - F_c^2)^2] / \sum(wF_o^2)^2\}^{1/2}$; $R(F) = \sum\Delta / \sum(F_o)$,
 $\Delta = |(F_o - F_c)|$; $w = [\sigma^2(F_o^2) + (aP)^2 + bP]^{-1}$; $P = [2F_c^2 + \text{Max}(F_o, 0)]/3$

Figure SI-1. Molecular diagram of $(\text{Ttz}^{\text{Ph,Me}})\text{ZnBr}$ (**3**) $\cdot 0.5\text{CH}_3\text{OH}$. Ellipsoids are shown at 30% probability. Hydrogen atoms are omitted for clarity. Selected bond lengths (\AA) and angles ($^\circ$): Zn-N1 2.036(2), Zn-Br 2.2713(8), N1-Zn-N1 91.86(6), N1-Zn-Br 123.93(5).

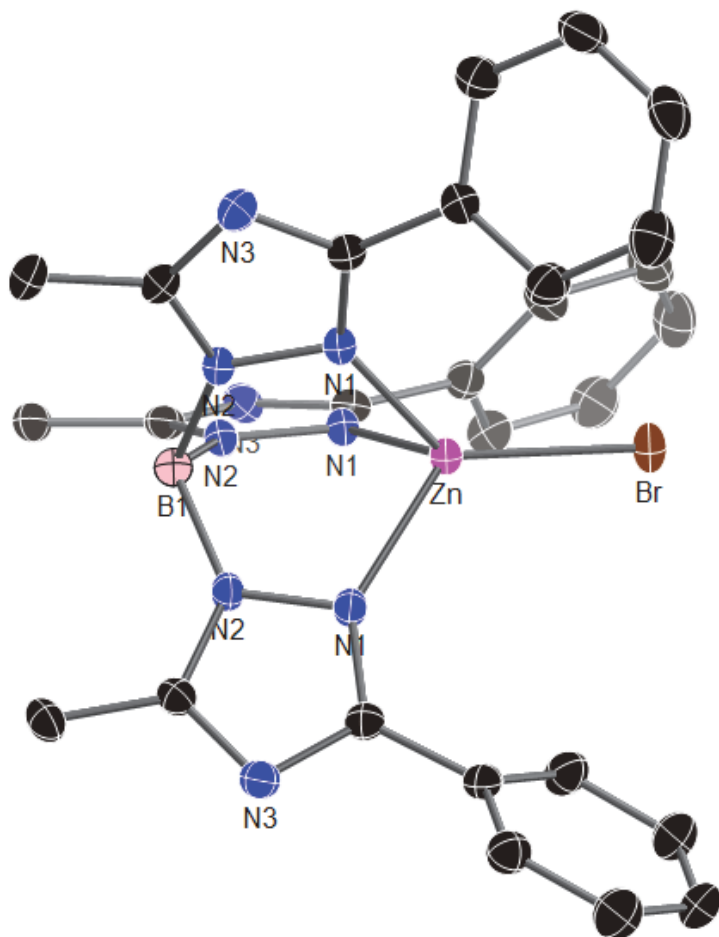


Figure SI-2. Molecular diagram of $(\text{Ttz}^{\text{Ph,Me}})_2\text{Zn}$ (**1_{Zn}**). Ellipsoids are shown at 30% probability. Hydrogen atoms are omitted for clarity.

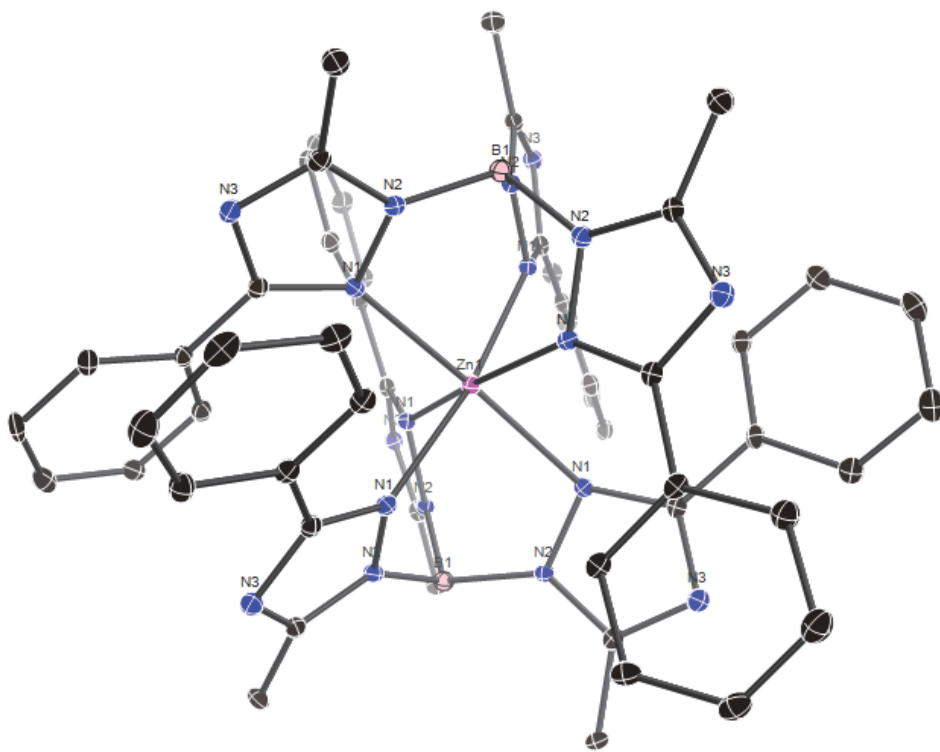


Figure SI-3. View down the B-M-B axis of various Ttz complexes. Color code: pink = B, blue = N, black = carbon. The metal atom is hidden by the B atom. In 1Ni* and 1Cu*, the rearranged Ph ring is circled in red.

1Ni* (bottom left is rearr Ph far away).

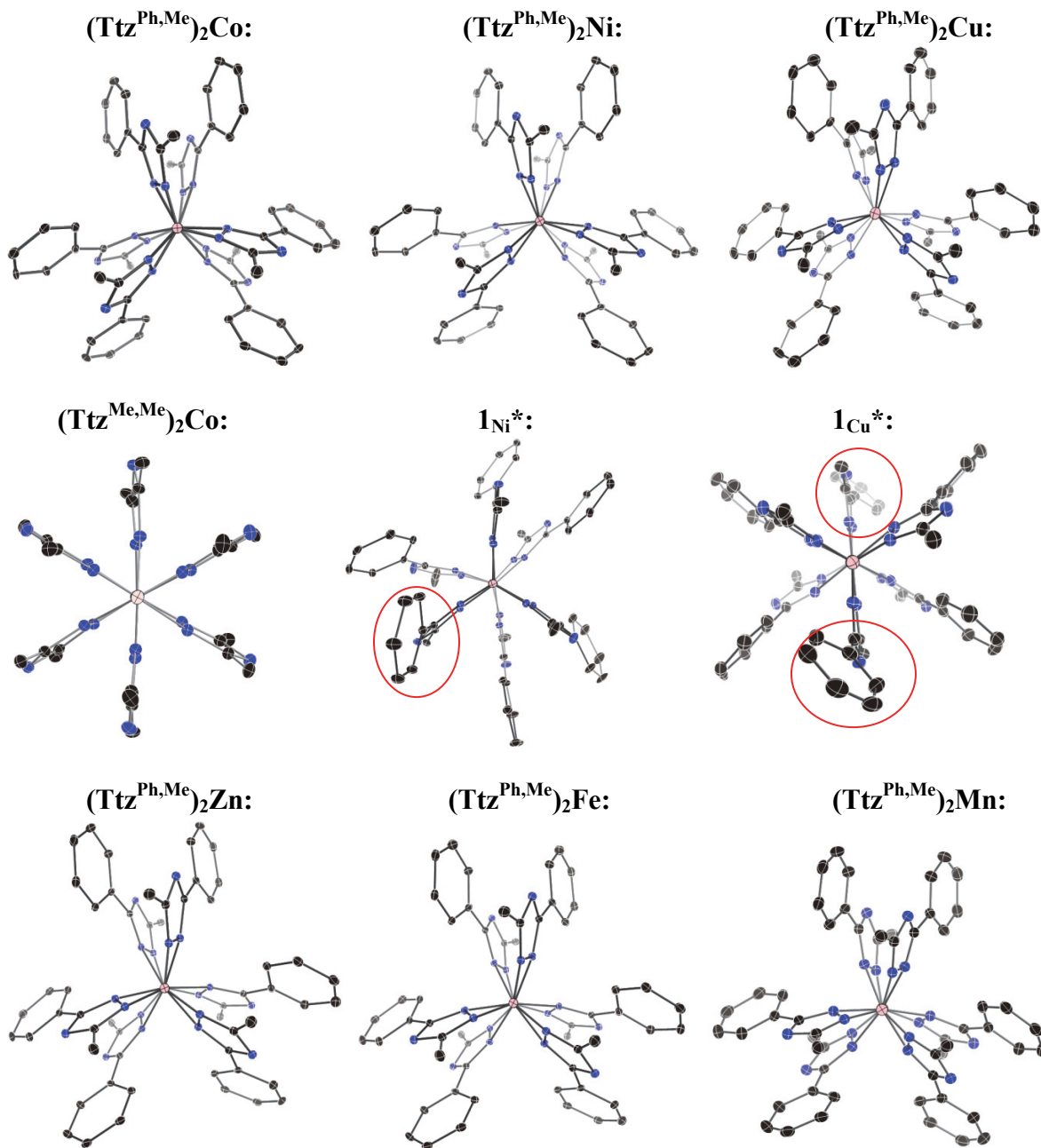


Figure SI-4. Temperature dependent NMR of the rearranged $(\text{Ttz}^{\text{Ph,Me}*})\text{Ni}(\text{Ttz}^{\text{Ph,Me}})$ complex. Inset: Plot of chemical shift vs. inverse temperature, only showing those that move with temperature. Those not included (C, E, F, H and J) showed no temperature dependence.

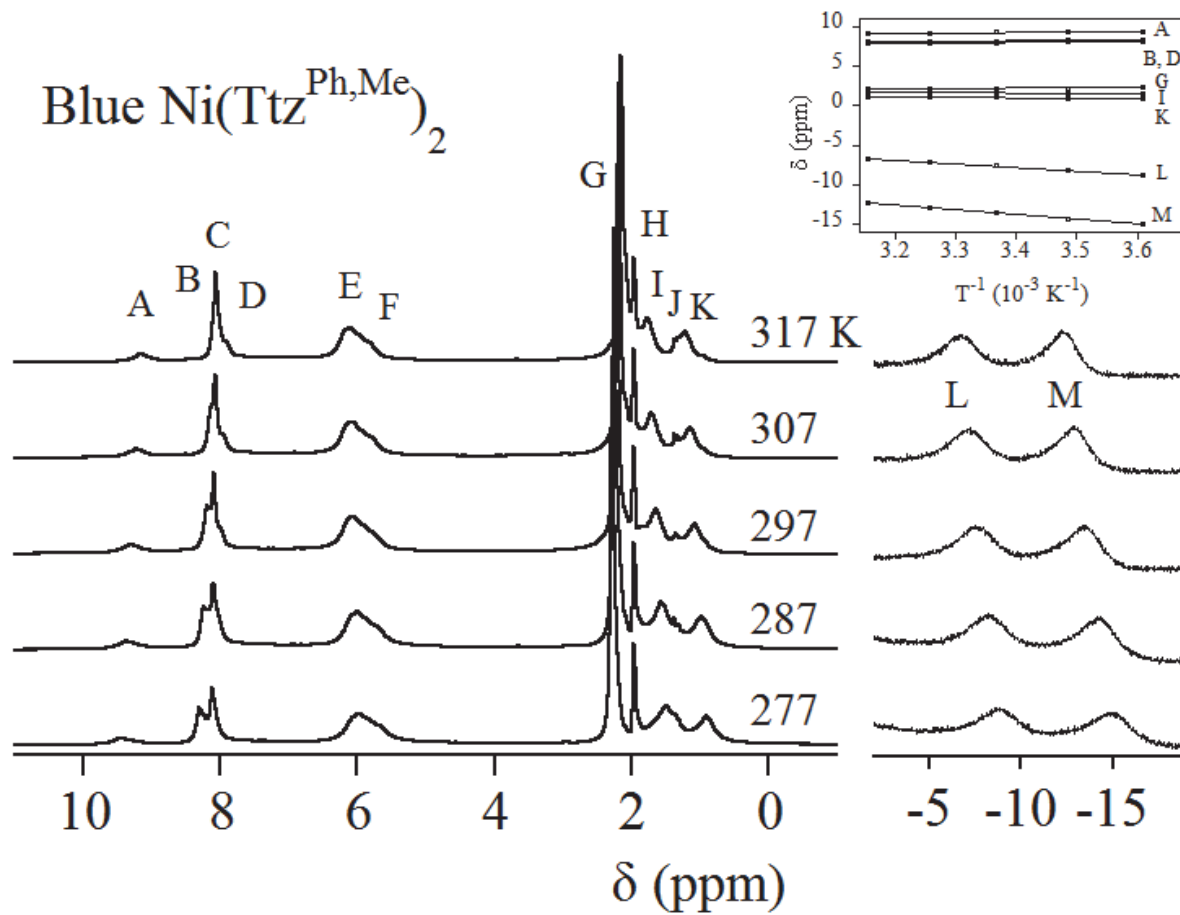


Figure SI-5. Molecular diagram of $(\text{Ttz}^{\text{Ph,Me}})_2\text{Fe}$ (**1_{Fe}**). Ellipsoids are shown at 30% probability. Hydrogen atoms are omitted for clarity.

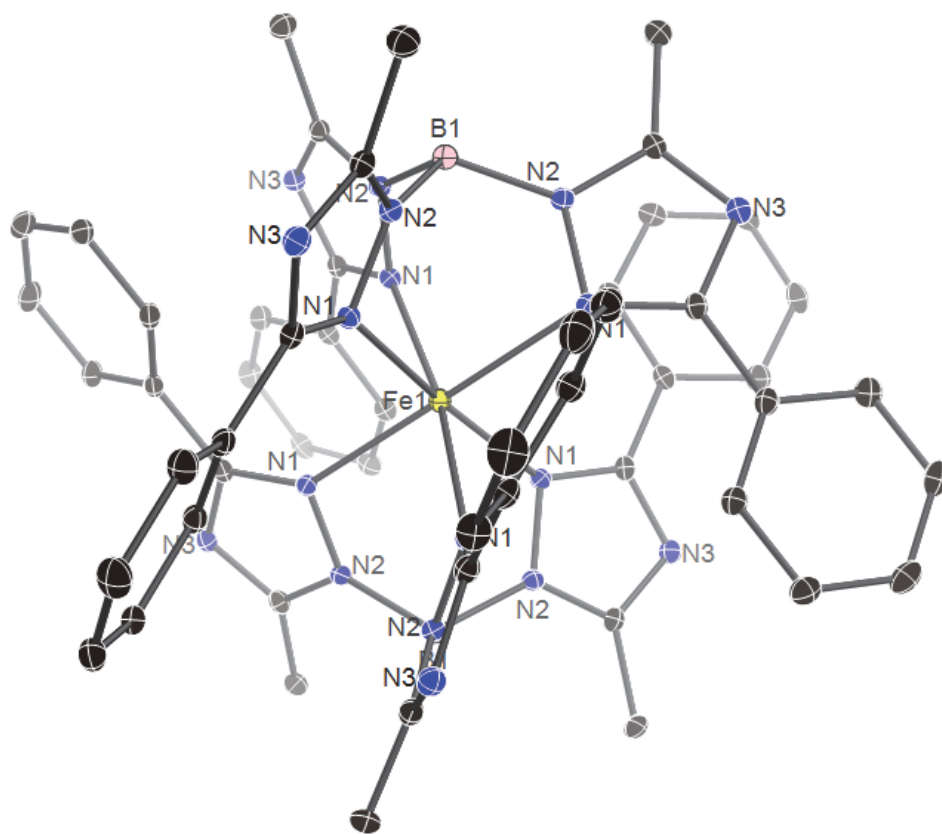


Figure SI-6. Molecular diagram of $(\text{Ttz}^{\text{Ph,Me}})_2\text{Mn}$ ($\mathbf{1}_{\text{Mn}}$). Ellipsoids are shown at 30% probability. Hydrogen atoms are omitted for clarity.

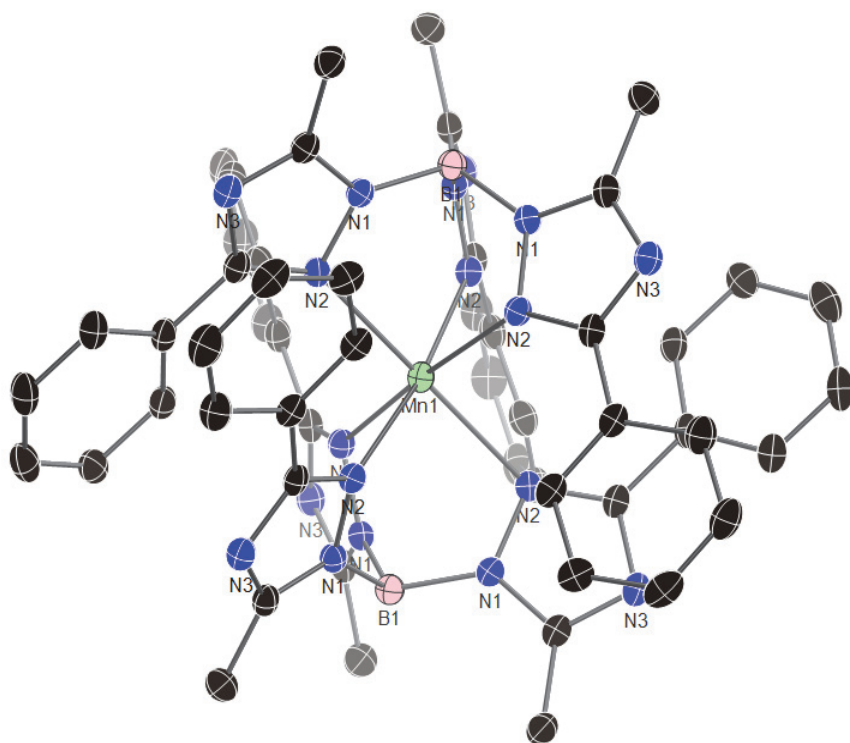


Figure SI-7. Coordination environment around the metal centers in $(\text{Ttz}^{\text{Ph,Me}})_2\text{M}$ ($\mathbf{1}_\text{M}$, $\text{M} = \text{Zn}$, Co , Fe , Mn).

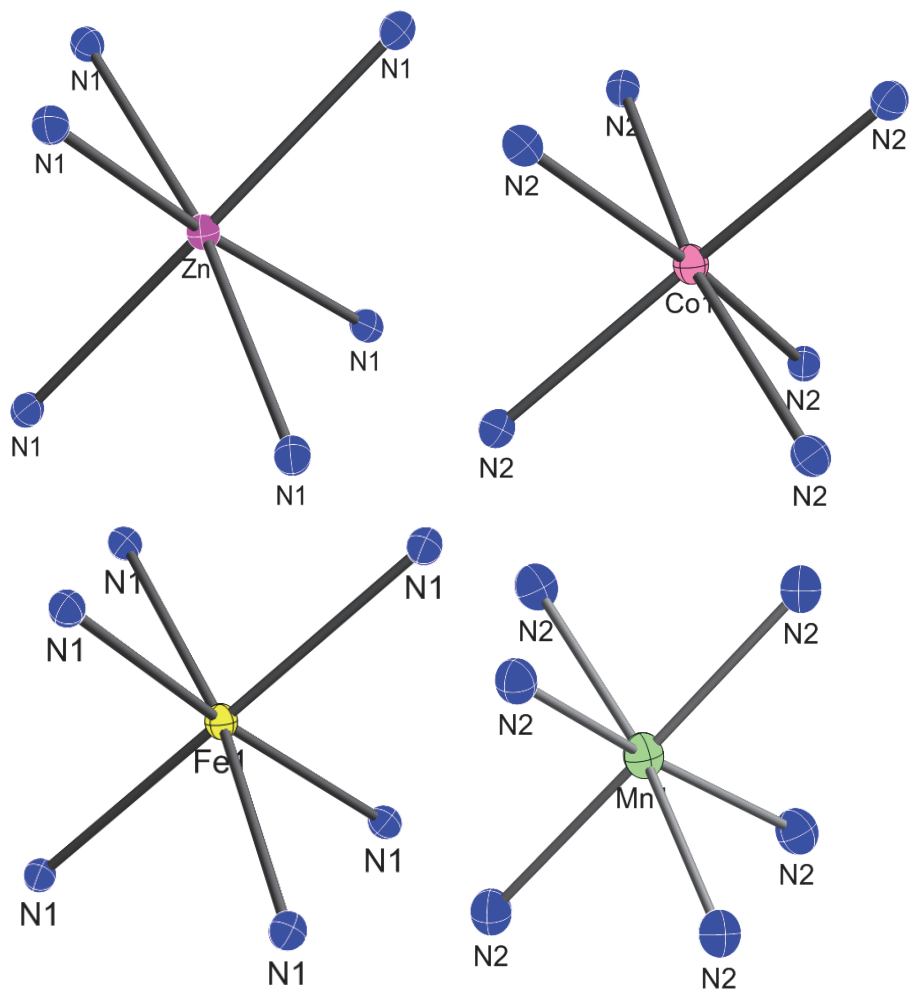


Figure SI-8. Comparison of observed (top) and predicted (bottom) powder patterns for $\text{Co}(\text{Ttz}^{\text{Ph,Me}})_2$.

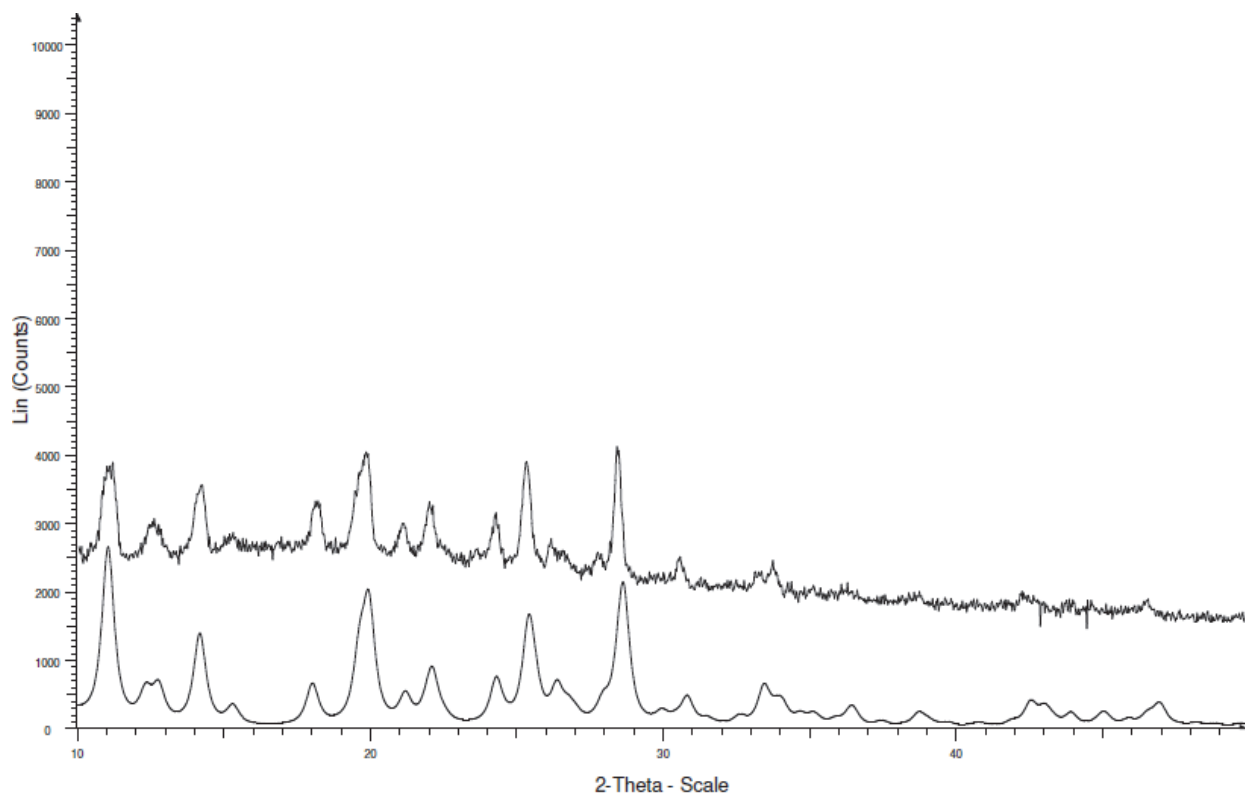


Figure SI-9. Comparison of observed (top) and predicted (bottom) powder patterns for $\text{Mn}(\text{Tz}^{\text{Ph,Me}})_2$.

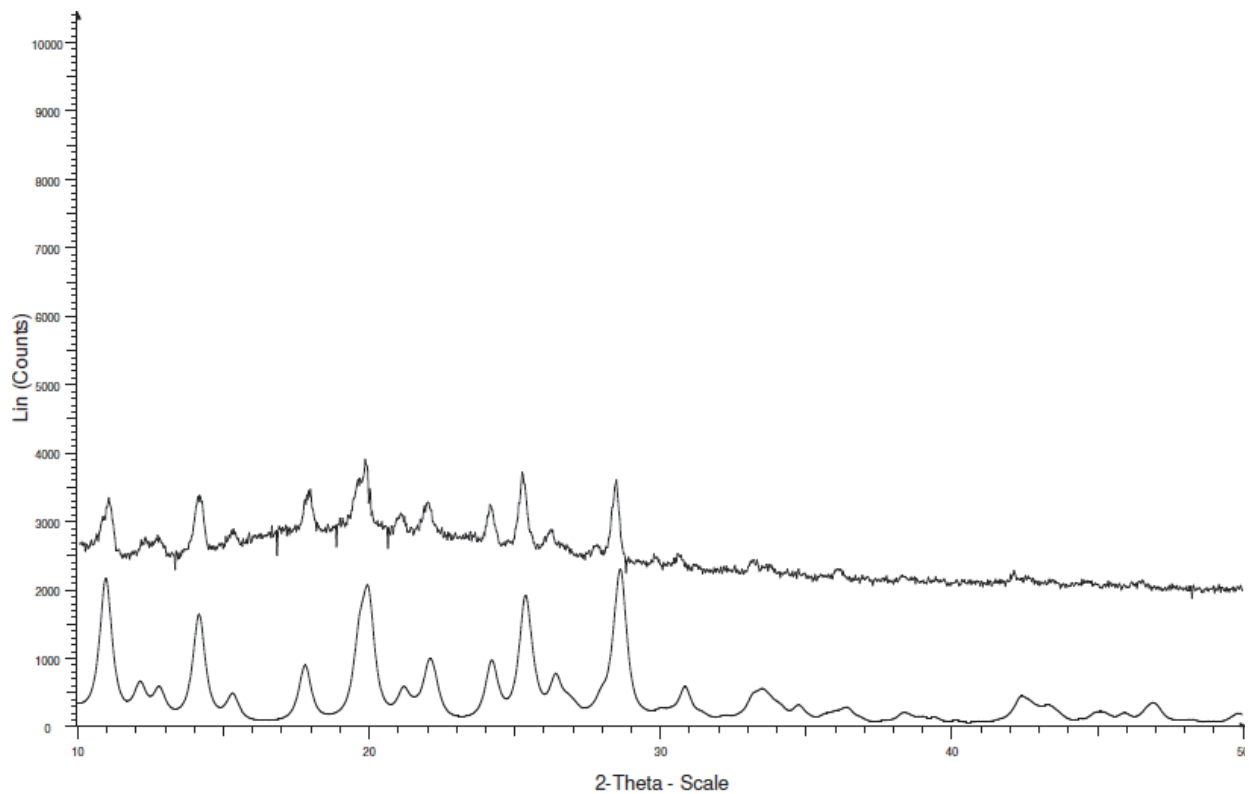


Figure SI-10. Comparison of observed (bottom) and predicted (top) powder patterns for $\text{Fe}(\text{Ttz}^{\text{Ph,Me}})_2$. Since the experimental powder pattern was obtained in air, some decomposition via oxidation of Fe is possible, and could account for imperfections in the fit.

